

Measurement of the Shape of the Transverse Momentum Distribution of W Bosons Produced in $p\bar{p}$ Collisions at $\sqrt{s} = 1.8$ TeV

B. Abbott,³¹ M. Abolins,²⁷ B. S. Acharya,⁴⁶ I. Adam,¹² D. L. Adams,⁴⁰ M. Adams,¹⁷ S. Ahn,¹⁴ H. Aihara,²³ G. A. Alves,¹⁰ N. Amos,²⁶ E. W. Anderson,¹⁹ R. Astur,⁴⁵ M. M. Baarmand,⁴⁵ L. Babukhadia,² A. Baden,²⁵ V. Balamurali,³⁵ J. Balderston,¹⁶ B. Baldin,¹⁴ S. Banerjee,⁴⁶ J. Bantly,⁵ E. Barberis,²³ J. F. Bartlett,¹⁴ A. Belyaev,²⁹ S. B. Beri,³⁷ I. Bertram,³⁴ V. A. Bezzubov,³⁸ P. C. Bhat,¹⁴ V. Bhatnagar,³⁷ M. Bhattacharjee,⁴⁵ N. Biswas,³⁵ G. Blazey,³³ S. Blessing,¹⁵ P. Bloom,⁷ A. Boehnlein,¹⁴ N. I. Bojko,³⁸ F. Borchering,¹⁴ C. Boswell,⁹ A. Brandt,¹⁴ R. Brock,²⁷ A. Bross,¹⁴ D. Buchholz,³⁴ V. S. Burtovoi,³⁸ J. M. Butler,³ W. Carvalho,¹⁰ D. Casey,²⁷ Z. Casilum,⁴⁵ H. Castilla-Valdez,¹¹ D. Chakraborty,⁴⁵ S.-M. Chang,³² S. V. Chekulaev,³⁸ L.-P. Chen,²³ W. Chen,⁴⁵ S. Choi,⁴⁴ S. Chopra,²⁶ B. C. Choudhary,⁹ J. H. Christenson,¹⁴ M. Chung,¹⁷ D. Claes,³⁰ A. R. Clark,²³ W. G. Cobau,²⁵ J. Cochran,⁹ L. Coney,³⁵ W. E. Cooper,¹⁴ C. Cretsinger,⁴² D. Cullen-Vidal,⁵ M. A. C. Cummings,³³ D. Cutts,⁵ O. I. Dahl,²³ K. Davis,² K. De,⁴⁷ K. Del Signore,²⁶ M. Demarteau,¹⁴ D. Denisov,¹⁴ S. P. Denisov,³⁸ H. T. Diehl,¹⁴ M. Diesburg,¹⁴ G. Di Loreto,²⁷ P. Draper,⁴⁷ Y. Ducros,⁴³ L. V. Dudko,²⁹ S. R. Dugad,⁴⁶ D. Edmunds,²⁷ J. Ellison,⁹ V. D. Elvira,⁴⁵ R. Engelmann,⁴⁵ S. Eno,²⁵ G. Eppley,⁴⁰ P. Ermolov,²⁹ O. V. Eroshin,³⁸ V. N. Evdokimov,³⁸ T. Fahland,⁸ M. K. Fatyga,⁴² S. Feher,¹⁴ D. Fein,² T. Ferbel,⁴² G. Finocchiaro,⁴⁵ H. E. Fisk,¹⁴ Y. Fisyak,⁴ E. Flattum,¹⁴ G. E. Forden,² M. Fortner,³³ K. C. Frame,²⁷ S. Fuess,¹⁴ E. Gallas,⁴⁷ A. N. Galyaev,³⁸ P. Gartung,⁹ V. Gavrilov,²⁸ T. L. Geld,²⁷ R. J. Genik II,²⁷ K. Genser,¹⁴ C. E. Gerber,¹⁴ Y. Gershtein,²⁸ B. Gibbard,⁴ S. Glenn,⁷ B. Gobbi,³⁴ A. Goldschmidt,²³ B. Gómez,¹ G. Gómez,²⁵ P. I. Goncharov,³⁸ J. L. González Solís,¹¹ H. Gordon,⁴ L. T. Goss,⁴⁸ K. Gounder,⁹ A. Goussiou,⁴⁵ N. Graf,⁴ P. D. Grannis,⁴⁵ D. R. Green,¹⁴ H. Greenlee,¹⁴ S. Grinstein,⁶ P. Grudberg,²³ S. Grünendahl,¹⁴ G. Guglielmo,³⁶ J. A. Guida,² J. M. Guida,⁵ A. Gupta,⁴⁶ S. N. Gurzhiev,³⁸ G. Gutierrez,¹⁴ P. Gutierrez,³⁶ N. J. Hadley,²⁵ H. Haggerty,¹⁴ S. Hagopian,¹⁵ V. Hagopian,¹⁵ K. S. Hahn,⁴² R. E. Hall,⁸ P. Hanlet,³² S. Hansen,¹⁴ J. M. Hauptman,¹⁹ D. Hedin,³³ A. P. Heinson,⁹ U. Heintz,¹⁴ R. Hernández-Montoya,¹¹ T. Heuring,¹⁵ R. Hirosky,¹⁷ J. D. Hobbs,⁴⁵ B. Hoeneisen,^{1,*} J. S. Hoftun,⁵ F. Hsieh,²⁶ Ting Hu,⁴⁵ Tong Hu,¹⁸ T. Huehn,⁹ A. S. Ito,¹⁴ E. James,² J. Jaques,³⁵ S. A. Jerger,²⁷ R. Jesik,¹⁸ J. Z.-Y. Jiang,⁴⁵ T. Joffe-Minor,³⁴ K. Johns,² M. Johnson,¹⁴ A. Jonckheere,¹⁴ M. Jones,¹⁶ H. Jöstlein,¹⁴ S. Y. Jun,³⁴ C. K. Jung,⁴⁵ S. Kahn,⁴ G. Kalbfleisch,³⁶ J. S. Kang,²⁰ D. Karmanov,²⁹ D. Karmgard,¹⁵ R. Kehoe,³⁵ M. L. Kelly,³⁵ C. L. Kim,²⁰ S. K. Kim,⁴⁴ B. Klima,¹⁴ C. Klopfenstein,⁷ J. M. Kohli,³⁷ D. Koltick,³⁹ A. V. Kostritskiy,³⁸ J. Kotcher,⁴ A. V. Kotwal,¹² J. Kourlas,³¹ A. V. Kozelov,³⁸ E. A. Kozlovsky,³⁸ J. Krane,³⁰ M. R. Krishnaswamy,⁴⁶ S. Krzywdzinski,¹⁴ S. Kuleshov,²⁸ S. Kunori,²⁵ F. Landry,²⁷ G. Landsberg,¹⁴ B. Lauer,¹⁹ A. Leflat,²⁹ H. Li,⁴⁵ J. Li,⁴⁷ Q. Z. Li-Demarteau,¹⁴ J. G. R. Lima,⁴¹ D. Lincoln,¹⁴ S. L. Linn,¹⁵ J. Linnemann,²⁷ R. Lipton,¹⁴ Y. C. Liu,³⁴ F. Lobkowicz,⁴² S. C. Loken,²³ S. Lökös,⁴⁵ L. Lueking,¹⁴ A. L. Lyon,²⁵ A. K. A. Maciel,¹⁰ R. J. Madaras,²³ R. Madden,¹⁵ L. Magaña-Mendoza,¹¹ V. Manankov,²⁹ S. Mani,⁷ H. S. Mao,^{14,†} R. Markeloff,³³ T. Marshall,¹⁸ M. I. Martin,¹⁴ K. M. Mauritz,¹⁹ B. May,³⁴ A. A. Mayorov,³⁸ R. McCarthy,⁴⁵ J. McDonald,¹⁵ T. McKibben,¹⁷ J. McKinley,²⁷ T. McMahan,³⁶ H. L. Melanson,¹⁴ M. Merkin,²⁹ K. W. Merritt,¹⁴ H. Miettinen,⁴⁰ A. Mincer,³¹ C. S. Mishra,¹⁴ N. Mokhov,¹⁴ N. K. Mondal,⁴⁶ H. E. Montgomery,¹⁴ P. Mooney,¹ H. da Motta,¹⁰ C. Murphy,¹⁷ F. Nang,² M. Narain,¹⁴ V. S. Narasimham,⁴⁶ A. Narayanan,² H. A. Neal,²⁶ J. P. Negret,¹ P. Nemethy,³¹ D. Norman,⁴⁸ L. Oesch,²⁶ V. Oguri,⁴¹ E. Oliveira,¹⁰ E. Oltman,²³ N. Oshima,¹⁴ D. Owen,²⁷ P. Padley,⁴⁰ A. Para,¹⁴ Y. M. Park,²¹ R. Partridge,⁵ N. Parua,⁴⁶ M. Paterno,⁴² B. Pawlik,²² J. Perkins,⁴⁷ M. Peters,¹⁶ R. Piegaia,⁶ H. Piekarczyk,¹⁵ Y. Pischalnikov,³⁹ B. G. Pope,²⁷ H. B. Prosper,¹⁵ S. Protopopescu,⁴ D. Pušeljčić,²³ J. Qian,²⁶ P. Z. Quintas,¹⁴ R. Raja,¹⁴ S. Rajagopalan,⁴ O. Ramirez,¹⁷ L. Rasmussen,⁴⁵ S. Reucroft,³² M. Rijssenbeek,⁴⁵ T. Rockwell,²⁷ M. Roco,¹⁴ P. Rubinov,³⁴ R. Ruchti,³⁵ J. Rutherford,² A. Sánchez-Hernández,¹¹ A. Santoro,¹⁰ L. Sawyer,²⁴ R. D. Schamberger,⁴⁵ H. Schellman,³⁴ J. Sculli,³¹ E. Shabalina,²⁹ C. Shaffer,¹⁵ H. C. Shankar,⁴⁶ R. K. Shivpuri,¹³ M. Shupe,² H. Singh,⁹ J. B. Singh,³⁷ V. Sirotenko,³³ W. Smart,¹⁴ E. Smith,³⁶ R. P. Smith,¹⁴ R. Snihur,³⁴ G. R. Snow,³⁰ J. Snow,³⁶ S. Snyder,⁴ J. Solomon,¹⁷ M. Sosebee,⁴⁷ N. Sotnikova,²⁹ M. Souza,¹⁰ A. L. Spadafora,²³ G. Steinbrück,³⁶ R. W. Stephens,⁴⁷ M. L. Stevenson,²³ D. Stewart,²⁶ F. Stichelbaut,⁴⁵ D. Stoker,⁸ V. Stolin,²⁸ D. A. Stoyanova,³⁸ M. Strauss,³⁶ K. Streets,³¹ M. Strovink,²³ A. Sznajder,¹⁰ P. Tamburello,²⁵ J. Tarazi,⁸ M. Tartaglia,¹⁴ T. L. T. Thomas,³⁴ J. Thompson,²⁵ T. G. Trippe,²³ P. M. Tuts,¹² N. Varelas,¹⁷ E. W. Varnes,²³ D. Vittoe,² A. A. Volkov,³⁸ A. P. Vorobiev,³⁸ H. D. Wahl,¹⁵ G. Wang,¹⁵ J. Warchol,³⁵ G. Watts,⁵ M. Wayne,³⁵ H. Weerts,²⁷ A. White,⁴⁷ J. T. White,⁴⁸ J. A. Wightman,¹⁹ S. Willis,³³ S. J. Wimpenny,⁹ J. V. D. Wirjawan,⁴⁸ J. Womersley,¹⁴ E. Won,⁴² D. R. Wood,³² H. Xu,⁵ R. Yamada,¹⁴ P. Yamin,⁴ J. Yang,³¹ T. Yasuda,³² P. Yepes,⁴⁰

C. Yoshikawa,¹⁶ S. Youssef,¹⁵ J. Yu,¹⁴ Y. Yu,⁴⁴ Z. Zhou,¹⁹ Z. H. Zhu,⁴² D. Zieminska,¹⁸ A. Zieminski,¹⁸
E. G. Zverev,²⁹ and A. Zylberstejn⁴³

(D0 Collaboration)

¹Universidad de los Andes, Bogotá, Colombia

²University of Arizona, Tucson, Arizona 85721

³Boston University, Boston, Massachusetts 02215

⁴Brookhaven National Laboratory, Upton, New York 11973

⁵Brown University, Providence, Rhode Island 02912

⁶Universidad de Buenos Aires, Buenos Aires, Argentina

⁷University of California, Davis, California 95616

⁸University of California, Irvine, California 92697

⁹University of California, Riverside, California 92521

¹⁰LAFEX, Centro Brasileiro de Pesquisas Físicas, Rio de Janeiro, Brazil

¹¹CINVESTAV, Mexico City, Mexico

¹²Columbia University, New York, New York 10027

¹³Delhi University, Delhi, India 110007

¹⁴Fermi National Accelerator Laboratory, Batavia, Illinois 60510

¹⁵Florida State University, Tallahassee, Florida 32306

¹⁶University of Hawaii, Honolulu, Hawaii 96822

¹⁷University of Illinois at Chicago, Chicago, Illinois 60607

¹⁸Indiana University, Bloomington, Indiana 47405

¹⁹Iowa State University, Ames, Iowa 50011

²⁰Korea University, Seoul, Korea

²¹Kyungshung University, Pusan, Korea

²²Institute of Nuclear Physics, Kraków, Poland

²³Lawrence Berkeley National Laboratory and University of California, Berkeley, California 94720

²⁴Louisiana Tech University, Ruston, Louisiana 71272

²⁵University of Maryland, College Park, Maryland 20742

²⁶University of Michigan, Ann Arbor, Michigan 48109

²⁷Michigan State University, East Lansing, Michigan 48824

²⁸Institute for Theoretical and Experimental Physics, Moscow, Russia

²⁹Moscow State University, Moscow, Russia

³⁰University of Nebraska, Lincoln, Nebraska 68588

³¹New York University, New York, New York 10003

³²Northeastern University, Boston, Massachusetts 02115

³³Northern Illinois University, DeKalb, Illinois 60115

³⁴Northwestern University, Evanston, Illinois 60208

³⁵University of Notre Dame, Notre Dame, Indiana 46556

³⁶University of Oklahoma, Norman, Oklahoma 73019

³⁷University of Panjab, Chandigarh 16-00-14, India

³⁸Institute for High Energy Physics, Protvino 142284, Russia

³⁹Purdue University, West Lafayette, Indiana 47907

⁴⁰Rice University, Houston, Texas 77005

⁴¹Universidade do Estado do Rio de Janeiro, Brazil

⁴²University of Rochester, Rochester, New York 14627

⁴³CEA, DAPNIA/Service de Physique des Particules, CE-SACLAY, Gif-sur-Yvette, France

⁴⁴Seoul National University, Seoul, Korea

⁴⁵State University of New York, Stony Brook, New York 11794

⁴⁶Tata Institute of Fundamental Research, Colaba, Mumbai 400005, India

⁴⁷University of Texas, Arlington, Texas 76019

⁴⁸Texas A&M University, College Station, Texas 77843

(Received 3 March 1998)

The shape of the transverse momentum distribution of W bosons (p_T^W) produced in $p\bar{p}$ collisions at $\sqrt{s} = 1.8$ TeV is measured with the D0 detector at Fermilab. The result is compared with QCD perturbative and resummation calculations over the p_T^W range from 0 to 200 GeV/ c . The shape of the distribution is consistent with the theoretical prediction. [S0031-9007(98)06465-5]

PACS numbers: 13.85.Qk, 12.38.Qk

The transverse momentum (p_T^W) of W intermediate vector bosons produced in proton-antiproton collisions is

due to the production of one or more gluons or quarks along with the boson. At low transverse momentum

($p_T^W < 10$ GeV/c), multiple soft gluon emission is expected to dominate the cross section. A soft gluon resummation technique [1–6] is therefore used to make QCD predictions. At high transverse momentum ($p_T^W > 20$ GeV/c), the cross section is dominated by the radiation of a single parton with large transverse momentum. Perturbative QCD [6] is therefore expected to be reliable in this regime. A prescription [4] has been proposed for matching the low and high p_T^W regions to provide a continuous prediction for all p_T^W . Thus, a measurement of the transverse momentum distribution may be used to check the soft gluon resummation calculations in the low p_T^W range, and to test the perturbative QCD calculations at high p_T^W .

The transverse momentum spectrum of W bosons has been measured previously by the UA1 [7], UA2 [8], and CDF [9] Collaborations, but with smaller data samples than the one used here. This paper presents a measurement of the shape of the p_T spectrum of W bosons produced in $p\bar{p}$ collisions at $\sqrt{s} = 1.8$ TeV with the D0 detector [10] at Fermilab, and extends the p_T^W range of the previous measurements. The data come from a sample of 12.4 ± 0.7 pb $^{-1}$ collected during the 1992–1993 run. A measurement of the inclusive cross section for W and Z boson production based on the same data set has been reported [11] and agrees with QCD predictions.

This measurement uses the decay mode $W \rightarrow e\nu$. Electrons were detected in a hermetic uranium–liquid-argon calorimeter with an energy resolution of about 15%/ \sqrt{E} (GeV). The calorimeter has a transverse granularity of $\Delta\eta \times \Delta\phi = 0.1 \times 0.1$, where η is the pseudorapidity and ϕ is the azimuthal angle. Electrons were accepted in the central pseudorapidity region only, $|\eta| < 1.1$, to keep the background contamination from multijet events at a reasonably low level for high values of p_T^W . The transverse momentum of the neutrino was calculated using the calorimetric measurement of the missing transverse energy (\cancel{E}_T) in the event. We take the p_T^W to be the sum of the electron and neutrino transverse momenta, measuring it only from the recoiling hadrons. The analysis used a single electron trigger, which required one electron with transverse energy (E_T) greater than 20 GeV.

The offline electron identification requirements consisted of four criteria: (i) the electron had to deposit at least 95% of its energy in the electromagnetic calorimeter (21 radiation lengths deep); (ii) the transverse and longitudinal shower shapes had to be consistent with those expected for an electron [12]; (iii) a good match had to exist between a reconstructed track in the drift chamber system and the shower position in the calorimeter; and (iv) the electron had to be isolated from other energy deposits in the calorimeter, with $I < 0.1$. This isolation variable is defined as $I = [E_{\text{TOT}}(0.4) - E_{\text{EM}}(0.2)]/E_{\text{EM}}(0.2)$, where $E_{\text{TOT}}(0.4)$ is the total calorimeter energy inside a cone of radius $\sqrt{\Delta\eta^2 + \Delta\phi^2} = 0.4$ and $E_{\text{EM}}(0.2)$ is the electromagnetic energy inside a cone of radius 0.2. To select the W boson candidate sample, we required one elec-

tron with $E_T > 25$ GeV and $\cancel{E}_T > 25$ GeV. Events having a second electron with $E_T > 20$ GeV that satisfies criteria (i), (ii), and (iv) were excluded from the candidate sample as possible $Z \rightarrow e^+e^-$ events. Criterion (iii) was not applied to this second electron in order to allow for possible tracking inefficiencies. These selection criteria yielded 7132 $W \rightarrow e\nu$ candidates.

The trigger and selection efficiencies were determined using $Z \rightarrow e^+e^-$ events in which one of the electrons satisfied the trigger and selection criteria. The second electron then provided an unbiased sample with which to measure the efficiencies. No dependence of the trigger or selection efficiency on p_T^W was found, to an accuracy of 5%.

A Monte Carlo program [13] was used to simulate the D0 detector response and calculate the kinematic and geometric acceptance as a function of p_T^W . The detector resolutions used in the Monte Carlo program were determined from data, and were parametrized as a function of energy and angle. The relative response of the hadronic and EM calorimeters was studied using the transverse momentum of the Z boson as measured by the p_T of the two electrons compared to the hadronic recoil system in the Z event. This parametrized representation of the D0 detector was used to smear the theoretical prediction by detector effects and compare it to our measured p_T^W . We prefer this method of comparison to a standard unfolding procedure [14] that proved to be sensitive to the choice of the prior distribution function. This sensitivity is caused by the Jacobian zero in dN/dp_T^W at the origin, which induces a peak that appears near $p_T^W \approx 4$ GeV/c after it is broadened by our p_T^W resolution. Only below 4 GeV/c do the true p_T^W distributions predicted by the two available models [4,5] exhibit a difference, which is masked in the data by these same resolution effects.

The dominant source of background in the W boson sample was multijet events where one or more of the jets fluctuated to fake an electron. Some multijet events also have significant \cancel{E}_T due to fluctuations and mismeasurements of the jet energies. This could fake a neutrino from W boson decay. The amount of multijet background in the $W \rightarrow e\nu$ candidate sample was determined by first defining a “loose” event sample which had the same selection criteria as the candidate sample except that electron identification criteria (i) and (ii) were not applied. This loose sample consisted of N_s signal events and N_b multijet background events. The $W \rightarrow e\nu$ candidate sample (described above) consisted of $\varepsilon_s N_s$ signal events and $\varepsilon_b N_b$ multijet background events, where ε_s and ε_b are the electron selection efficiencies for the candidate relative to the loose samples, for signal and background, respectively. We obtained ε_s from the $Z \rightarrow e^+e^-$ sample, and ε_b from events with $\cancel{E}_T < 15$ GeV. The total multijet background was determined to be $(4.2 \pm 2.3)\%$. The shape of the multijet background as a function of p_T^W was determined by repeating the procedure in different p_T^W bins.

To cross-check the multijet background estimate, the transverse mass and the \cancel{E}_T distributions of the final data sample were compared to a model of the expected distributions obtained from a combination of $W \rightarrow e\nu$ Monte Carlo events plus the estimated multijet background. The comparison was performed in three p_T^W bins: 0–30 GeV/c, 30–60 GeV/c, and >60 GeV/c; the number of $W \rightarrow e\nu$ candidates in each bin was 6726, 282, and 124. The amount of multijet background in each p_T^W bin was estimated as $(2.9 \pm 1.6)\%$, $(20.9 \pm 11.7)\%$, and $(38.3 \pm 21.5)\%$, respectively. Figure 1 shows the results of the comparisons. The distinctive shape of the transverse mass distribution for multijet background arises from applying the kinematic cuts and the minimum p_T^W requirement to a sample predominantly composed of dijet events that lie back-to-back in the transverse plane. The goodness of the fit between the data and the model is evaluated by performing a χ^2_λ test [15]. The numerical results for $\chi^2_\lambda/\text{d.o.f.}$ for each fit in Fig. 1 are (a) 20.2/25, (b) 26.4/19, (c) 4.7/7, (d) 5.4/9, (e) 3.0/13, and (f) 2.1/7. They correspond to fit probabilities of (a) 74%, (b) 12%, (c) 69%, (d) 80%, (e) 99%, and (f) 95%, respectively. We therefore conclude that the tests show good agreement between the data and the expectation.

The normalized multijet background was subtracted bin by bin from the W boson candidate sample transverse momentum spectrum. Additional corrections (all less than 5%) were made to account for top quark background

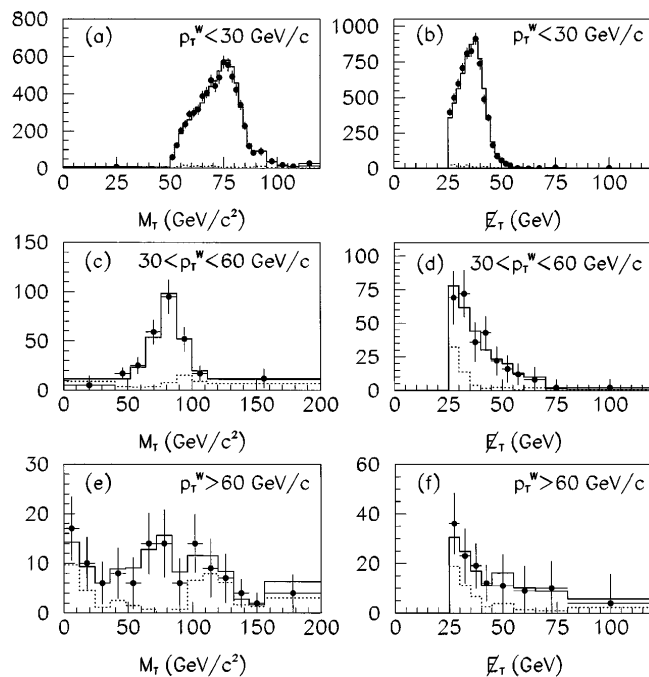


FIG. 1. The transverse mass (left) and \cancel{E}_T (right) distributions for three p_T^W bins. The points are the D0 data. The solid histogram is the sum of the Monte Carlo signal and the estimated background. The dotted histogram is the estimated background alone.

events and for $Z \rightarrow e^+e^-$ events where one of the electrons was lost or not identified. Since p_T^W was measured from the recoiling hadrons, the events originating from $W \rightarrow \tau\nu$ (where $\tau \rightarrow e\nu\nu$) contributed properly to the differential distribution; this source of background therefore was included in the Monte Carlo simulation of the p_T^W distribution.

The normalized distribution of the W boson transverse momentum ($\frac{1}{N} \frac{dN}{dp_T^W}$) is shown in Fig. 2 and given in Table I. The largest contributions to the systematic error in the p_T^W measurement are the uncertainty in the magnitude of the multijet background, the uncertainty in the hadronic recoil energy scale factor and resolution used in the detector simulation, and the uncertainty in the selection efficiency. These are all added in quadrature since they are independent. We compare our experimental result to the theoretical prediction [4] computed using the MRSA' [16] parton distribution function and smeared for detector resolutions. The variation of the theoretical prediction for various parton distribution functions is negligible. The measurement and the prediction are independently area normalized to unity. These points are used to perform a more detailed comparison between data and theory by plotting the ratio (data-theory)/theory, which is shown in Fig. 3. At low p_T^W (< 60 GeV/c), where the statistical errors are small but the detector resolution

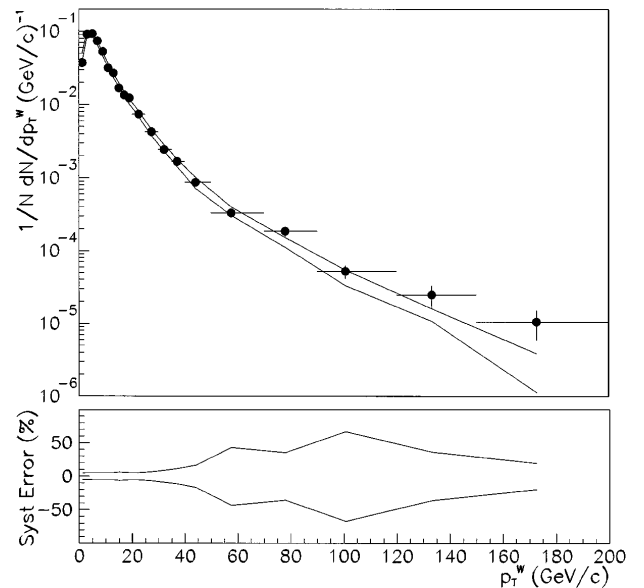


FIG. 2. The W boson transverse momentum spectrum, showing the D0 result (solid points) with statistical uncertainty. The theoretical calculation by Arnold and Kauffman [4], smeared for detector resolutions, is shown as two lines corresponding to the $\pm 1\sigma$ variations of the uncertainties in the detector modeling. Within each bin, the values are plotted at the mean p_T^W . The fractional systematic uncertainty on the data is shown as a band in the lower portion of the plot. The values of the uncertainties for different p_T^W bins are 100% correlated with each other. Upward fluctuations in the magnitude of the multijet background cause the widening observed in the band at about 60 and 100 GeV/c in p_T^W .

TABLE I. The W boson transverse momentum distribution corresponding to Fig. 2. The column labeled “Stat. error” shows the statistical uncertainty; “Syst. error” shows the systematic uncertainty in background and efficiency; “Detector error” shows the systematic uncertainty in the detector modeling; “Total error” is the sum in quadrature of the previous three columns.

Bin width (GeV/c)	$\langle p_T^W \rangle$ (GeV/c)	N_{signal}	$(1/N) (dN/dp_T^W)$ (c/TeV)	Stat. error (c/TeV)	Syst. error (c/TeV)	Detector error (c/TeV)	Total error (c/TeV)
2	1.2	506.8	37.4	1.6	1.9	6.1	6.6
2	3.0	1232.0	90.8	2.6	4.6	7.9	9.5
2	5.0	1253.0	92.4	2.6	4.8	4.4	7.0
2	7.0	1006.6	74.2	2.3	3.9	3.7	5.8
2	9.0	718.4	53.0	1.9	2.8	2.6	4.2
2	11.0	431.2	31.8	1.5	1.7	2.0	3.0
2	13.0	368.4	27.2	1.4	1.4	1.6	2.6
2	15.1	228.0	16.8	1.1	1.1	1.2	1.9
2	17.1	184.4	13.6	1.0	0.8	0.8	1.5
2	19.0	167.9	12.4	0.9	0.7	0.9	1.5
5	22.6	252.0	7.43	0.46	0.42	0.65	0.89
5	27.3	145.4	4.29	0.34	0.30	0.43	0.61
5	32.3	83.0	2.45	0.25	0.22	0.26	0.42
5	37.2	56.7	1.67	0.20	0.19	0.18	0.33
10	44.2	59.4	0.875	0.099	0.147	0.150	0.232
20	57.7	45.2	0.333	0.037	0.144	0.045	0.155
20	78.0	25.2	0.186	0.028	0.066	0.020	0.075
30	100.7	10.7	0.052	0.011	0.035	0.010	0.038
30	133.2	5.1	0.025	0.008	0.009	0.002	0.013
50	172.7	3.6	0.011	0.005	0.002	0.001	0.005

effects dominate the result, the data are encompassed by the systematic error band. This agreement persists at high p_T^W (> 60 GeV/c) but with larger statistical errors. A quantitative comparison of data and theory in the high

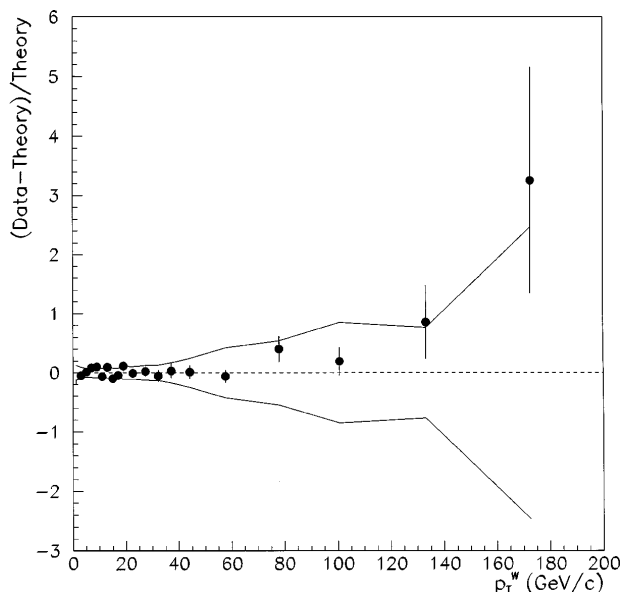


FIG. 3. The ratio (data-theory)/theory shown as a function of p_T^W with its statistical uncertainty as error bars. Within each bin, the values are plotted at the mean p_T^W . The theory corresponds to Ref. [4], smeared for detector resolutions. The systematic uncertainties from data (background and efficiency) and from the detector modelling are added in quadrature and shown as a band.

p_T^W region shows that the two agree when the correlations in the systematic errors are properly taken into account. We therefore conclude that the shape of the distribution is consistent with the theoretical prediction.

In summary, we have measured the shape of the transverse momentum distribution of W bosons produced in $p\bar{p}$ collisions at $\sqrt{s} = 1.8$ TeV, and have found that it is consistent with the combined QCD perturbative and resummation calculations.

We thank the staffs at Fermilab and collaborating institutions for their contributions to this work, and acknowledge support from the Department of Energy and National Science Foundation (U.S.A.), Commissariat à l’Energie Atomique (France), State Committee for Science and Technology and Ministry for Atomic Energy (Russia), CAPES and CNPq (Brazil), Departments of Atomic Energy and Science and Education (India), Colciencias (Colombia), CONACyT (Mexico), Ministry of Education and KOSEF (Korea), and CONICET and UBA-CyT (Argentina).

*Visitor from Universidad San Francisco de Quito, Quito, Ecuador.

†Visitor from IHEP, Beijing, China.

- [1] J. Collins, D. Soper, and G. Sterman, Nucl. Phys. **B250**, 199 (1985); J. Collins and D. Soper, Nucl. Phys. **B193**, 381 (1981); Nucl. Phys. **B197**, 446 (1982); Nucl. Phys. **B213**, 545(E) (1983).
- [2] C. Davies, B. Webber, and W.J. Stirling, Nucl. Phys. **B256**, 413 (1985); C. Davies and W.J. Stirling, Nucl. Phys. **B244**, 337 (1984).

-
- [3] G. Altarelli, R.K. Ellis, M. Greco, and G. Martinelli, Nucl. Phys. **B246**, 12 (1984).
- [4] P.B. Arnold and R. Kauffman, Nucl. Phys. **B349**, 381 (1991).
- [5] G.A. Ladinsky and C.P. Yuan, Phys. Rev. D **50**, 4239 (1994).
- [6] P.B. Arnold and M.H. Reno, Nucl. Phys. **B319**, 37 (1989); R.J. Gonsalves, J. Pawlowski, and C-F. Wai, Phys. Rev. D **40**, 2245 (1989).
- [7] UA1 Collaboration, C. Albajar *et al.*, Z. Phys. C **44**, 15 (1989).
- [8] UA2 Collaboration, J. Alitti *et al.*, Z. Phys. C **47**, 523 (1990).
- [9] CDF Collaboration, F. Abe *et al.*, Phys. Rev. Lett. **66**, 2951 (1991); Phys. Rev. Lett. **67**, 2937 (1991).
- [10] D0 Collaboration, S. Abachi *et al.*, Nucl. Instrum. Methods Phys. Res., Sect. A **338**, 185 (1994).
- [11] D0 Collaboration, S. Abachi *et al.*, Phys. Rev. Lett. **75**, 1456 (1995).
- [12] D0 Collaboration, S. Abachi *et al.*, Phys. Rev. D **52**, 4877 (1995).
- [13] D0 Collaboration, B. Abbott *et al.*, Fermilab-Pub-97/328-E, hep-ex/9710007, 1997 (to be published); Fermilab-Pub-97/422-E, hep-ex/9712029, 1997 (to be published).
- [14] G. D'Agostini, Nucl. Instrum. Methods Phys. Res., Sect. A **362**, 487 (1995).
- [15] S. Baker and R.D. Cousins, Nucl. Instrum. Methods Phys. Res., Sect. A **221**, 437 (1984).
- [16] A.D. Martin, R.G. Roberts, and W.J. Stirling, Phys. Rev. D **50**, 6734 (1994); **51**, 4756 (1995).